Photoreversible Dark State in a Tristable Green Fluorescent Protein Variant

Riccardo Nifosì, Aldo Ferrari, Caterina Arcangeli, Valentina Tozzini, Vittorio Pellegrini,* and Fabio Beltram

NEST-INFM and Scuola Normale Superiore, I-56100 Pisa, Italy

Received: August 5, 2002; In Final Form: October 21, 2002

The reversible photoinduced structural changes of a green fluorescent protein (GFP) mutant and their optical control are reported. A photoreversible optically inactive configuration is demonstrated with the absorption peak at 365 nm, which is consistent with a photoisomerization pathway associated with hydrogen-bond breaking in the chromophore environment. We show that this state is involved in the switching dynamics recently discovered in these molecules and we determine the transition rates of the reversible photoconversion processes. These experiments combine to provide the framework for the implementation and optimization of efficient room-temperature GFP-based all-optical memories that use the fluorescent properties of these proteins.

Introduction

The availability of distinct photoconvertible states is the key feature of photochromic molecules.[1] Probing and understanding photoconversion processes is a central issue in modern photochemistry and is currently stimulating a broad research effort. From a more applicative point of view, optical control of the molecular structure represents a viable strategy to store and manipulate data at high spatial resolution. In particular biomolecules such as proteins, peptides and DNA represent promising building blocks[2−4] that can lead to innovative routes toward photonics at the nanoscale. These molecules offer naturally evolved structures and can be further optimized by genetic engineering. In this way they allow the implementation of unique bioelectronic devices to specification and may lead to short-term applications in diagnostics and pharmaceutics thanks to the structure−function relation of these biomolecules and their controlled sensitivity to the environment. One example is that of bacteriorhodopsin. The understanding of its chemical-physical properties and of the microscopic pathways linking its photocycle intermediates[5,6] opened the way to an important research effort to investigate its device applications. Bacteriorhodopsin-based volumetric optical memories were proposed which exploit photoisomerization between distinct chromophore states populated during the photochemical cycle and were shown to offer great potential for data storage.[7] Bacteriorhodopsin efficiently photoisomerizes but does not fluoresce, making its use impossible in schemes involving single-molecule detection and access. Yet this ultimate regime represents the strategy of choice toward electronics and photonics at the nanoscale.

In this paper we investigate the photoconversion dynamics and the states involved in a strongly fluorescent biomolecule belonging to the green fluorescent protein (GFP) family and identify the nonfluorescent dark chromophore state C involved in the photoconversion process. GFP-class fluorophores are characterized by two stable configurations A and B that differ in protonation.[8] We demonstrate that C is distinct from A and B and absorbs at higher energies. In addition we argue that the photoconversion mechanism requires the reorganization of hydrogen bonds between the chromophore and the rest of the protein. We also measure the average number of photons required to toggle the molecular structure between states A/B and C. Our data and analysis are supported by molecular-dynamics and ab initio calculations and by a series of experiments in which optical control of the fluorescent emission is shown with proteins immobilized in aqueous polymer gels with different values of laser intensity and irradiation times.

GFPs are intrinsically fluorescent molecules whose optical properties are determined by a photoexcitable green-light emitter chromophore autocatalytically generated by the posttranslational modification of a 3-amino acid sequence (Ser65−Tyr66−Gly67).[9] This chromophore consists of the hydroxybenzyl side chain of Tyr66 (phenolic ring) and the imidazolidinone ring formed by cyclization of the tripeptide (heteorocyclic ring). It is positioned in a cavity containing a number of neighboring polar and aromatic residues. These are important in establishing a hydrogen-bond network around the chromophore involving also some water molecules. GFP fluorescence and absorption critically depend on this network and perturbation of the latter can induce marked variations in GFP photophysics.

The absorption spectrum of wild-type GFP (wt-GFP) exhibits two peaks at 395 and 475 nm associated with distinct ionization states of the chromophore identified with neutral (state A) and anionic (state B) states, respectively.[10] The emission peak is at 508 nm and originates from recombination from the excited B state. Photoconversion between neutral and anionic states is associated with a proton-transfer mechanism within a picosecond time scale.[11] GFP mutants designed for intensified fluorescence, modified spectral characteristics, photostability, and other advantageous properties are also available and have found significant applications in biological studies as optical markers to monitor protein function.[8,12,13]

GFP fluorescence dynamics is characterized by transitions between fluorescent (bright) and nonfluorescent (dark) states. At the single-molecule level these lead to reversible turning on and off (blinking) and ultimate switching off (photobleaching) of the emission[14,15] in a few-second time scale. In addition, faster excitation-driven changes in the optical emission in the sub-milliseconds time scale were recently observed.[16] This complex single-molecule behavior triggered a large effort aimed at modeling the molecular structure of the states involved in blinking and photobleaching and the photochemical mechanisms by which they are accessed. The nature of the dark states is

* Corresponding author. E-mail: vp@nest.sns.it.

10.1021/jp0266852 CCC: $25.00
Published on Web 01/24/2003

still a debated issue, however, and the available photophysical models fail to fully account for the fluorescence dynamics of each mutant.

The availability of these distinct ground states stimulated the exploitation of GFPs to store and manipulate data at the single-molecule level. To that end, however, efficient control of the photoconversion between different states is required, a process that was first discovered in yellow-fluorescent GFP mutants incorporating mutations at position 203 (S65G/S72A/T203Y and S65G/S72A/T203F).[17] In these mutants dark to bright photoconversion was achieved by irradiation at 405 nm for 5 min at an intensity of 1 W/cm^2 and was proposed to involve the neutral and anionic states as dark and bright states. In EGFP (Enhanced GFP, a widely used high-brightness marker characterized by mutations F64L/S65T), we demonstrated that control of photoconversion between dark and bright states was not achievable by irradiation at frequencies different from that of the excitation laser at 476 nm.[18] However, the specific point mutation T203Y (threonin in tyrosin at position 203 in the amino acid sequence) in the EGFP amino acidic structure was sufficient to enable the optical control of these transitions. Contrary to the observations in the yellow-fluorescent molecules, the optical control of EGFP-T203Y (in the following, E^{2}GFP) was demonstrated down to the ultimate limit of single molecules with two lasers at 476 nm (photobleaching) and 350 nm (dark to bright photoconversion), but not at 405 nm (i.e., in resonance with state A absorption).[19]

Materials and Methods

Optical Spectroscopy. The GFP variants EGFP (F64L/S65T) and E^{2}GFP (F64L/S65T/T203Y) were a gift of Dr. Mudit Tyagi (International Centre of Genetic Engineering and Biotechnology, Trieste, Italy) and Prof. Mauro Giacca (NEST-INFM and Scuola Normale Superiore, Pisa, Italy). EGFP and E^{2}GFP absorption spectra were measured using an UV/Vis spectrometer (Lambda 25, Perkin-Elmer; scan rate of absorption spectra 240 nm/min, spectral bandwidth 2.0 nm). For these experiments recombinant proteins were diluted in PBS (phosphate buffer solution) to a final concentration of 1 g/L. GFPs entrapped in the pores of PAA gel were prepared from 1 g/L solutions of protein. PAA gels (T = 15%, C = 3% without sodium dodecyl sulfate; catalysis, tetramethylenediamine and ammonium persulfate) were prepared in pH 7 phosphate saline buffer (Gibco brl, Life Technologies) doped with protein (here T is the total concentration of monomer in grams per 100 mL, C is the wt % of total monomer, which is *N*,*N*′-methylenebis(acrylamide)). The gel host provided a pore size small enough for convenient immobilization of each protein molecule or clusters of molecules while their naturally fluorescent and native conformation was maintained.[18] Each sample consisted of an 8 μL aliquot that polymerized rapidly between the glass cover slip and remained optically transparent, giving PAA gel films about 10 μm thick with protein densities of 5−200 ng/cm^2. These gels were analyzed by an optical system based on epifluorescence, giving the possibility of studying both the spectral properties and the spatial distribution of the molecules. Illuminations at wavelengths between 514 and 350 nm were provided by an argon-ion (Stabilite 2017, Spectra-Physics) and an argon/krypton ion laser (Beamlock, Spectra-Physics). The two lasers were focused onto a circular field of view of about 7 μm^2 in PAA gels by a 100 × 1.3 numerical aperture oil-immersion objective. GFP molecules were imaged by an intensified CCD (PentaMax Princeton Instruments; 0.1 s integration time).

Computational Modeling. Molecular dynamics simulations were performed with the Amber6 force field and simulation package.[20] The solvated protein was simulated at constant temperature (300 K) and pressure (1 atm). The starting structure for the neutral cis state was built by homology modeling from X-ray structures of various GFP mutants, as described in ref 21. The initial configuration of the neutral trans state was obtained by a 180° rotation around the double bond of the cis chromophore of a thermalized structure. To remove close contacts between the trans chromophore and its environment, very small time steps were used in the beginning following the procedure adopted by Weber et al.[22] The force-field parameters for the chromophore were set following the standard parametrization in Amber.[21] The charges were derived by fitting the electrostatic potential of a model chromophore and the geometric parameters obtained from a structure minimized using density-functional theory.[23] The same method was used for ab initio calculations of the chromophore in the presence of polar functional groups modeling the protein environment.

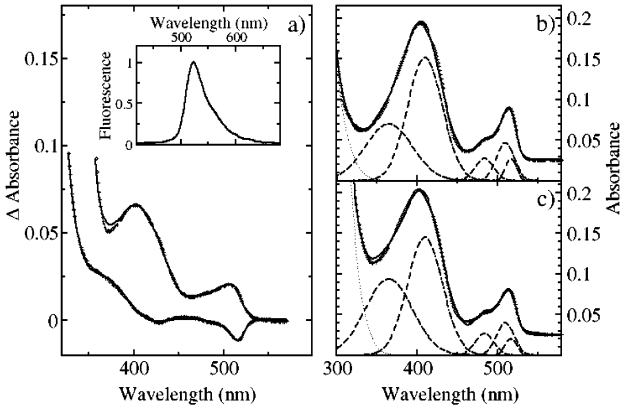

Figure 1. (a) Differential absorbance (i.e., absorbance (t = 8 h) − absorbance (t = 0)) after excitation at 476 nm (102 mW, 1.4 W/cm^2 lower curve) and after excitation at 350 nm (20 mW, 0.28 W/cm^2 upper curve) (open dots = data, line = fit). The scan rate of absorption spectra is 240 nm/min and the spectral bandwidth is 2.0 nm. The inset shows room-temperature fluorescence spectrum of T203Y-EGFP (E^{2}GFP) at 2 mM in PBS, pH = 7.0 after excitation at 476 nm (102 mW, 1.4 W/cm^2). (b) and (c) Absorption spectra at 2 mM in PBS, pH = 7.0 before (b) and after (c) laser excitation at 476 nm (102 mW, 1.4 W/cm^2) for t = 8 hours. The solid and dashed curves are the result of the Gaussian fit and its spectral decomposition, respectively. The dotted curves fit the high-energy part of the spectrum and are due to aromatic amino acids not linked to chromophore dynamics.

Results and Discussion

Observation of the Dark State. The inset of Figure 1a shows the room-temperature emission spectrum of E^{2}GFP at pH = 7 following excitation at 476 nm. At this pH both A and B states are populated (measured pK_a value is 7.2, data not shown). Due to the T203Y mutation, the emission is red-shifted (from 508 to 525 nm) compared to wt-GFP and EGFP.[24] Radiative recombination of state A at ∼450 nm is extremely weak (data not shown). To investigate the existence of a third populated state following photobleaching, we monitored the evolution of E^{2}GFP absorption at pH = 7 before (Figure 1b) and after (Figure 1c) irradiation at 476 nm (1.4 W/cm^2) for 8 h. Measurements were performed in PBS at concentration 1 g/L at room temperature. Analysis of the data was performed by decomposing the absorption spectra as a sum of Gaussian curves (dashed lines in Figure 1b,c). The three peaks close to 515 nm are associated with three vibrational levels of the anionic state (B) and the broad peak centered at 410 nm with the neutral state (A). We observe that at 476 nm the absorption of state A is one-tenth of the total measured value at that frequency. An

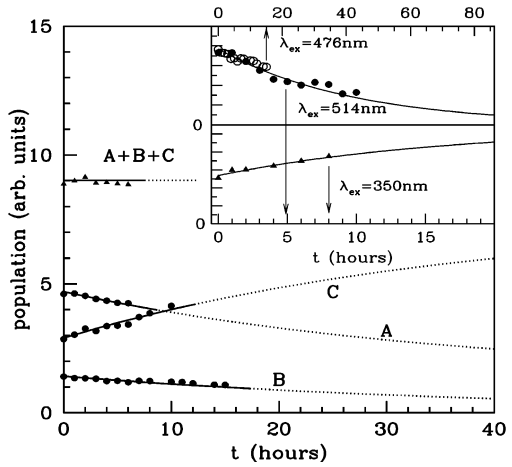

Figure 2. Populations of states A (band at 410 nm), B (515 nm), and C (365 nm) as a function of photobleaching time (i.e., irradiation at 476 nm with 102 mW/cm^2 to 1.4 W/cm^2). For each state, the population was evaluated from the integral of the corresponding Gaussian curve resulting from the spectral decomposition (for B the sum of the absorption of the three vibrational states was taken) and reported as dots in the main graph. Triangles represent the measured total population as the sum of A, B, and C contributions. The lines are multiexponential fits based on a closed model system of three states connected by first-order dynamics. The (constant) sum of the three states population is also shown. Extrapolated values are represented as dotted lines. Inset: Changes of B populations during photobleaching at 476 nm (upper part, open dots), photobleaching at 514 nm (185 mW, 2.6 W/cm^2) (upper part, filled dots), and photoconversion at 350 nm (20 mW, 0.28 W/cm^2) (lower part, triangles), together with the fits resulting from the three-state model.

additional peak at 365 nm (hereafter called C) is clearly observed. The tail in the UV part of the spectrum was fitted with a Gaussian centered at around 270 nm (dotted lines in Figure 1b,c). Comparison of the two spectra reveals that the suppression of the absorption of states A and B after irradiation at 476 nm associates with a significant increase of population of state C, an effect that is not observed in EGFP where state C absorption is absent (data not shown). To substantiate this conclusion, we report in Figure 1a representative differential absorption spectra (Absorption(t) − Absorption(t=0) at t = 8 h) following illumination at 476 nm (lower curve) and 350 nm at 0.28 W/cm^2 (upper curve). The data display a drastically different behavior. In the first case, photobleaching of states A and B correlates with the appearance of the feature at 365 nm associated with state C, whereas in the second case an efficient repopulation of states A and B can be observed (upper curve in Figure 1a). The light-induced increase of the absorption spectra below 300 nm stems from contributions of aromatic amino acids[25] that are not linked to chromophore dynamics, as suggested by the fact that the sum of the population of the three states A, B, and C remains constant as a function of time (see triangles in Figure 2a). In conclusion, the data reported in Figure 1 demonstrate that light-induced conversion occurs in E^{2}GFP and involves the three states A, B, and C.

Reversible Photoconversion and Transition Rates. The decomposition of the absorption spectra in distinct peaks reported in Figure 1 allows us to evaluate the rates of change of population of A, B, and C. These parameters crucially determine the intrinsic dynamics of the switching mechanism. The observed behavior is reported in Figure 2. The main panel displays the evolution of states A, B, and C following photobleaching, i.e., the values of the integrated absorption of the three states following excitation at 476 nm with 1.4 W/cm^2 (dots are the experimental values). This phenomenology is consistently described by a closed three-level system governed by a first-order dynamics. Each transition is described by a rate constant k (i.e., the inverse of the transition time τ) given by $k = p\ \mathrm{d}N/\mathrm{d}t$, where p is the intrinsic probability of the process and $\mathrm{d}N/\mathrm{d}t$ is the number of absorbed photons per unit time per protein ($\mathrm{d}N/\mathrm{d}t = I\sigma/h\upsilon$, I is the incident light intensity at frequency υ and σ is the absorption cross section). The fit of the population behavior as a function of time based on this model is shown in the main panel of Figure 2 by the solid lines and gives an accurate description of the experimental results. The inset of Figure 2 reports the evolution of state B following photobleaching due to excitation at 514 with 2.6 W/cm^2 (top panel, filled dots) and photoconversion due to excitation at 350 nm with 0.28 W/cm^2 (bottom panel, triangles). Solid lines represent the fit. Taking into account excitation intensities and absorption cross sections, the evolution of state B depopulation is independent of the excitation wavelength, and the data corresponding to different excitation frequencies scale onto the same exponential (see top panel of inset where data corresponding to excitation at 476 nm are also reported as open dots).

From these results, the characteristic decay (or recovery) times of state B (and consequently of the fluorescence) can be evaluated. These times strongly depend on the excitation intensities, and on the ratio between the total volume of the GFP solution (80 mm^3) and that irradiated by the laser light (12 mm^3).[26] Decay times of the order of many hours ($\tau \sim 10$ h and $\tau \sim 35$ h for the C → B and B → C transitions, respectively) are observed for the values used in our experiments. Taking into account these factors and the GFP absorption cross section, the average number of photons necessary to induce the transitions (i.e., $1/p$) for a single E^{2}GFP molecule can be deduced: $n_C \sim 1 \times 10^6$ and $n_B \sim 9 \times 10^6$ for C → B and B → C transitions, respectively. These fluence per molecule values set the optically controlled switching dynamics of the protein and, for a given laser intensity, determine the excitation time required for the switching to occur.

Read, Write, and Erase Operations with Immobilized Proteins. To further investigate E^{2}GFP photophysics and show how read−erase−write operations can be carried out at different excitation times and intensities, molecules immobilized in polyacrylamide gels were directly imaged and photobleached by excitation at 476 nm and then photoactivated by excitation at 350 nm. We selected small clusters of a few tens of molecules trapped in gels to reduce the impact of statistical fluctuations. Figure 3 (upper panel) shows a sequence of E^{2}GFP switching behavior, with photoactivation times of 2.5 s, 1 s, and 250 ms (from left to right) and intensity of 60 kW/cm^2. Photobleaching (erase procedure) was achieved by 7.7-s-long illumination with an argon laser (intensity 1 kW/cm^2) centered at 476 nm. The lower panel of Figure 3 reports the amount of fluorescence recovery at different UV irradiation times (from 0.25 to 2.5 s) and laser intensities (0.6, 1.8, and 60 kW/cm^2). The dependence of photoconversion to the bright state on UV intensities and irradiation times is consistent with the behavior observed in solutions. According to the fluence per molecule n_r reported above, efficient photoconversion can be achieved at 0.6 kW/cm^2 for excitation times exceeding 2.5 s, whereas at 1.8 kW cm^2 this time decreases to 0.8 s. This trend is reproduced in our experiments with immobilized proteins where a substantial decrease of photoconversion efficiency is found at around 2 and 1 s at these two power intensities. With the highest intensity (corresponding to 4.6 mW at 350 nm focused onto an area of approximately 3 μm diameter) the bright state could be reproducibly recovered in the whole range of exposure times

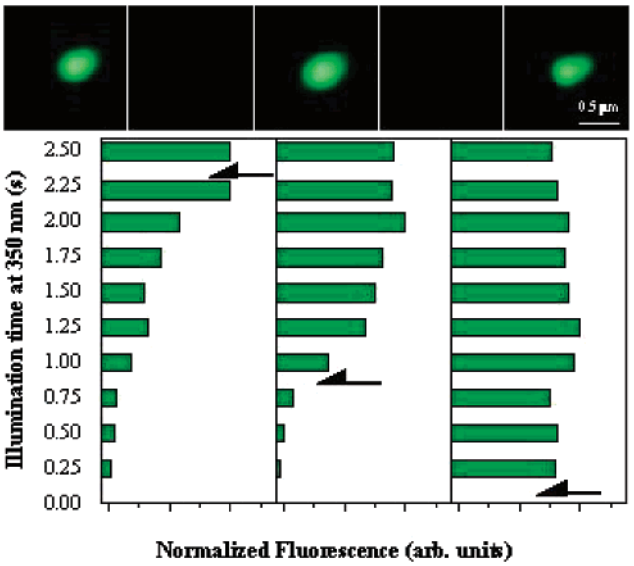

Figure 3. Write−read−erase operations illustrated by a series of experiments performed on clusters of E^2GFP molecules trapped in polyacrylamide PAA gel films (10 μm thick). The upper panel shows a representative sequence of E^2GFP switching behavior, with photoactivation times (write process) of 2.5 s, 1 s, and 250 ms (from the left to the right) at 350 nm (60 kW/cm^2). Erase processes are accomplished by 7.7 s excitation at 476 nm (1 kW/cm^2). The green histograms in the lower panels report the integrated fluorescence intensity of E^2GFP clusters after 350 nm laser illumination at different laser powers: 0.05 mW (0.6 kW/cm^2, leftmost panel), 0.14 mW (1.8 kW/cm^2, center panel), and 4.6 mW (60 kW/cm^2, rightmost panel) as a function of irradiation time (from 0.25 to 2.5 s). E^2GFP molecules were imaged (read process) by an intensified charge coupled device (CCD) camera (0.1 s integration time) during irradiation at 476 nm. Black arrows indicate the irradiation times for efficient photoconversion as deduced from the data in solution.

(more than 10^2 read−erase−write cycles were performed). This is consistent with the fact that the estimated time required for the switching from C to B (write procedure) at this intensity is about 25 ms. To our knowledge, these results show for the first time the switching dynamics of these proteins and clarify operational limits for information storage, readout, and manipulation within an all-optical scheme. These experiments also indicate that by tuning laser power and irradiation times, different percentages of photoconverted proteins can be obtained by hinting at more complex storage schemes when memory cells comprise many proteins.

Photophysical Model. Figure 4a shows a schematic representation of the three main states of E^2GFP together with the relevant transitions (dashed and solid arrows) and absorption/emission wavelengths as resulting from the experiments. The question arises, what are the microscopic molecular mechanisms underlying these reversible photoconversion processes? The key observation is that C-state absorption occurs at higher energy with respect to that of (neutral) state A. Two factors can be responsible for the observed absorption energy shift in E^2GFP, namely, variation of the protonation state of the chromophore and changes in the interaction with the protein environment. A number of recent calculations showed that zwitterionic, cationic, and anionic forms lead to absorption energies *below* that of the neutral form.[23,27] This indicates that state C corresponds to a neutral chromophore. Distinct neutral chromophore configurations, however, do not differ in energy gaps appreciably,[22] and a dominant role must be played by the chromophore environment. To investigate this, we performed ab initio calculations adding one by one the three hydrogen bonds between the (neutral) chromophore and the protein, i.e., the two donors on the O2 carboxyl oxygen (Gln94 and Arg96) and the acceptor on the phenolic oxygen (a water molecule). We found that each hydrogen-bond interaction does result in a substantial red shift consistently with previous theoretical studies.[27,28] In particular, the energy gap of the isolated neutral chromophore was calculated at an energy above the measured absorption energy in the protein.[27] We conclude that state C involves a less coordinated neutral chromophore and that hydrogen-bond breaking in the environment occurs with photoconversion.

This analysis, however, does not uniquely identify the photoconversion process leading to the observed phenomenology. A particularly attractive mechanism is based on cis−trans photoisomerization, a light-induced rotation around the double bond connecting the two rings of the chromophore. In this case the C state corresponds to a trans isomer of the neutral chromophore. This mechanism was proposed by Weber et al.[22] to explain the weak fluorescence of state A. Such weak fluorescence signals (at 450 nm and at 525 nm) were observed also for E^2GFPs after resonant excitation of state A (at 405 nm) in agreement with other experiments on T203Y variants.[29] We wish to stress that other configurations of the environment with suppressed hydrogen bonds could be considered for the C state. In particular, external protonation of the chromophore may occur through the facing His148 residue. Once this proton transfer takes place, the hydrogen bond with the close water molecule could become unstable, thus yielding a neutral state with the required reduced hydrogen-bond coordination. Further experiments and simulations are needed to identify the structural properties of the dark C state and to clarify the most favorable pathway of photoconversion.

As shown in the following, however, the cis−trans isomerization mechanism meets the requirements for the observed photoconversion process. Indeed, though the energy difference of absorption between trans and cis configurations of the *isolated* chromophore is expected to be extremely small,[22] this transformation does induce a modification of the hydrogen-bond network. As shown by the molecular dynamics calculations reported in Figure 4, the hydrogen bond between Gln94 and the O2 oxygen of the chromophore breaks after 20 ps of simulation of the *trans*-chromophore configuration as required to blue shift the absorption energy (see the two chromophore configurations in Figure 4 bottom panel). Within this model, a possible mechanism for population of the C state, i.e., the trans-isomer, is the direct excitation and subsequent nonradiative decay of state A, which still has a significant absorption at 476 nm as deducible from the Gaussian deconvolution in Figure 1. Alternatively, the event may start with protonation of the chromophore occurring in the excited B state. This process is energetically disfavored, because it is known that the neutral chromophore becomes more acidic in the excited state,[28] but nevertheless it was proposed to be involved in the photophysics of the EGFP variant.[26] The reverse on-switching process is straightforward, because in this case the trans-neutral state is directly excited at 350 nm, and the tran−cis photoisomerization repopulates state A. The light-driven conversion across the ground-state barrier[30] ensures a fast equilibration of the A and B species, completing the picture of reactivation from C to B.

Conclusions

In this work we demonstrated the existence of a photoreversible optically inactive configuration (dark state C) with peak absorption at 365 nm in an EGFP variant with mutation T203Y. We have elucidated the switching dynamics connecting bright and dark states and associated it with reorganization of the

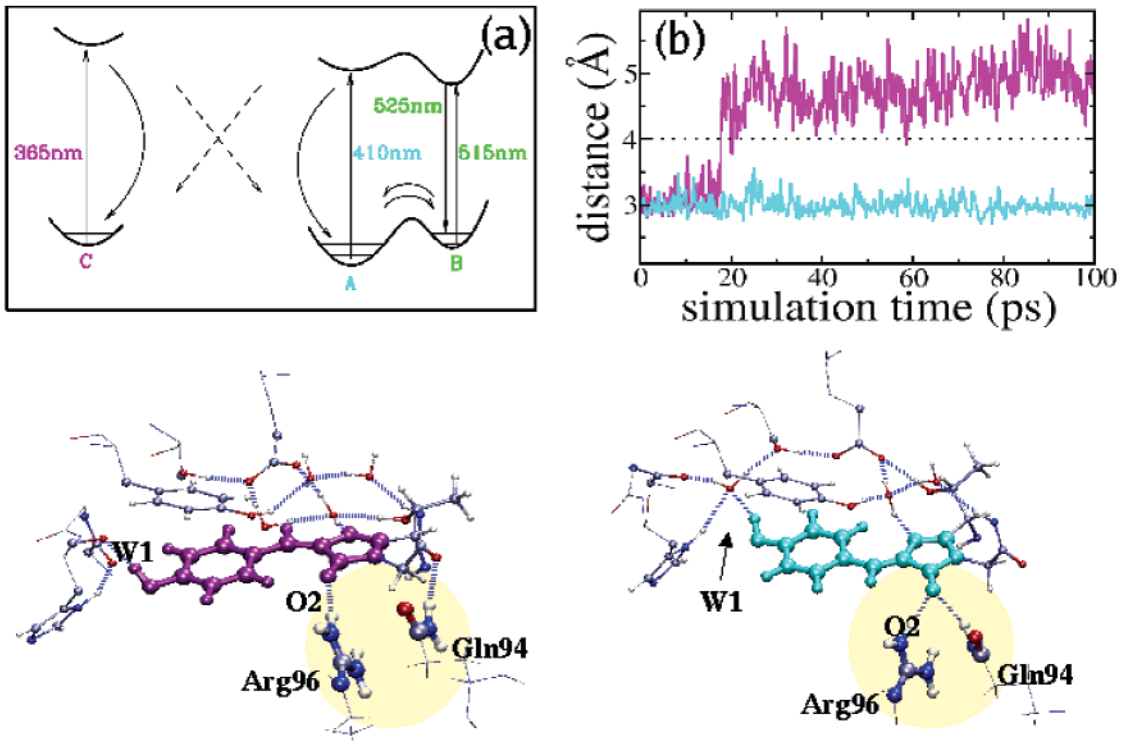

Figure 4. Panel a: schematic representation of the three main states in E^{2}GFP. Vertical arrows represent absorption/emission processes between vibrational levels in ground and excited states. Dashed arrows are used to indicate the transition process between bright and dark states. A ground-state barrier crossing between A and B is also indicated. Panel b: distance between O2 of the chromophore and the donor of Gln94 reported during the first 100 ps of the simulation for the trans state (magenta line) and of the cis state (cyan line), the sudden increase in the distance indicating the breaking of the hydrogen bond. Lower panel: structures of the chromophore and its environment in E^{2}GFP for neutral cis state (right) and neutral trans state (left) as obtained from molecular dynamics simulations.

hydrogen-bond network. Consequently, we suggested possible pathways for the switching mechanism. We believe that the working model for E^{2}GFP photophysics and the observed dynamics of the conversion process can be precious tools to guide further optimization of GFP by mutagenesis for specific applications. One example is their use as building blocks for the implementation of high-density all-optical memory architectures.[17,18] In particular, mutations able to modify the hydrogen-bond contacts of one or both states could yield larger separation between the characteristic absorption wavelengths of A and C. This will allow more efficient photobleaching (erase process) by resonant excitation of A. Optical-memory elements that exploit the peculiar photophysics of these proteins show great promise because they are photochemically stable at room temperature, offer three photoconnected states addressable down to the single-molecule level, and display optical control with wavelengths, power, and times suggestive of prototype technological implementation. To this end, further studies aimed at addressing the impact of blinking events on the ultimate speed of operation of such devices need to be carried out. E^{2}GFP and other mutants that display controllable photochromism may also find new applications in biology where prolonged monitoring of protein function in living cells is required. Specific mutations that can adjust the environment sensitivity of the optical properties,[31] the folding efficiency and can tailor pK_a values to allow monitoring of GFP-tagged molecules in acid conditions should be carried out and may open further new opportunities for future research in molecular and cell biology.

Acknowledgment. We thank Mauro Giacca and Mudit Tyagi for GFP production and Paolo Faraci for technical assistance. This work was supported by grants from MIUR (Ministero dell'Università e della Ricerca Scientifica e Tecnologica), from INFM/B (Istituto Nazionale per la Fisica della Materia, section B), and INFM's Parallel Computing Initiative.

References and Notes

(1) *Photo-Reactive Materials for Ultrahigh-Density Optical Memory*; Irie, M, Ed.; Elsevier: Amsterdam, 1994.
(2) Benenson, Y.; Paz-Elizur, T.; Adar, R.; Keinan, E.; Livneh, Z.; Shapiro, E. *Nature* **2001**, *414*, 430−434.
(3) Whaley, S. R.; English, D. S.; Hu, E. L.; Barbara, P. F.; Belcher, A. M. *Nature* **2000**, *405*, 665−658.
(4) Braun, E.; Eichen, Y.; Sivan, U.; Ben-Yoseph, G. *Nature* **1998**, *391*, 775−758.
(5) Chizhov, I.; Chernavskii, D. S.; Engelhard, M.; Mueller, K. H.; Zubov, B. V.; Hess, B. *Biophys. J.* **1996**, *71*, 2329−2345.
(6) Haupts, U.; Tittor, J.; Oesterhelt, D. *Annu. Rev. Biophys. Biomol. Struct.* **1999**, *28*, 367−399. Kobayoshi, T.; Saito, T.; Ohtani, H. *Nature* **2001**, *414*, 531−534.
(7) Birge, R. R.; Gillespie, M. B.; Izaguirre, E. W.; Kuznetzow, A.; Lawrence, A. F.; Singh, D.; Wang Song, Q.; Schmidt, E.; Stuart, J. A.; Seetharaman, S.; Wise, K. J. *J. Phys. Chem. B* **1999**, *103*, 10746−10766.
(8) Tsien, R. *Annu. Rev. Biochem.* **1998**, *67*, 509−544.
(9) Heim, R.; Prasher, D. C.; Tsien, R. Y. *Proc. Natl. Acad. Sci. U.S.A.* **1994**, *91*, 12501−12504.
(10) Brejc, K.; Sixma, T. K.; Kitts, P. A.; Kain, S. R.; Tsien, R. Y.; Ormö, M.; Remington, S. J. *Proc. Natl. Acad. Sci. U.S.A.* **1997**, *94*, 2306−2311.
(11) Chattoraj, M.; King, B. A.; Bublitz, G. U.; Boxer S. G. *Proc. Natl. Acad. Sci. U.S.A.* **1996**, *93*, 8362−8367.
(12) Green fluorescent protein. In *Methods in Enzimology 302*; Conn, P. M., Ed.; Academic Press: San Diego, 1999.
(13) Phair, R. D.; Misteli, T. *Nature* **2000**, *404*, 604−609.
(14) Pierce, D. W.; Hom-Booher, N.; Vale, R. D. *Nature* **1997**, *388*, 338.
(15) Garcia-Parajo, M. F.; Segers-Nolten, G. M. J.; Veerman J.-A.; Greve J.; van Hulst, N. F. *Proc. Natl. Acad. Sci. U.S.A.* **2000**, *97*, 7237−7242.
(16) Schwille, P.; Kummer, S.; Heikal, A. A.; Moerner, W. E.; Webb, W. W. *Proc. Natl. Acad. Sci. U.S.A.* **2000**, *97*, 151−156.
(17) Dickson, R. M.; Cubitt, A. B.; Tsien, R. Y.; Moerner, W. E. *Nature* **1997**, *388*, 355−358.

(18) Cinelli, R. A. G.; Ferrari, A.; Pellegrini, V.; Tyagi, M.; Giacca, M.; Beltram, F. *Photochem. Photobiol*. **2000**, *71*, 771−776.
(19) Cinelli, R. A. G.; Pellegrini, V.; Ferrari, A.; Faraci, P.; Nifosì, R.; Tyagi, M.; Giacca, M.; Beltram, F. *Appl. Phys. Lett*. **2001**, *79*, 3353−3355.
(20) Case, D.; Pearlman, D.; Caldwell, J.; Cheatham, T., III; Ross, W.; Simmerling, C.; Darden, T.; Merz, K.; Stanton, R.; Cheng, A.; Vincent, J.; Crowley, M.; Tsui, V.; Radmer, R.; Duan, Y.; Pitera, J.; Massova, I.; Seibel, G.; Singh, U.; Weiner P.; Kollman, P. A. Amber 6.0, 1999.
(21) Nifosì, R.; Tozzini, V. *Proteins*, in press.
(22) Weber, W.; Helms, V.; McCammon, J. A.; Langhoff, P. W. *Proc. Natl. Acad. Sci. U.S.A.* **1999**, *96*, 6177−6182.
(23) Tozzini, V.; Nifosì, R. *J. Phys. Chem. B* **2001**, *105*, 5797−5803.
(24) Ormö, M.; Cubitt, A. B.; Kallio, K.; Gross, L. A.; Tsien, R. Y.; Remington, S. J. *Science* **1996**, *273*, 1392−1395.
(25) Lackowicz, J. R. *Principle of fluorescence spectroscopy*, 2nd ed.; Kluwer Academic: New York, 1999.
(26) Haupts, U.; Maiti, S.; Schwille P.; Webb, W. W. *Proc. Natl. Acad. Sci. U.S.A.* **1998**, *95*, 13573−13578.
(27) Voityuk, A. A.; Kummer, A. D.; Michel-Beyerle, M. E.; Rosch, N. *Chem. Phys.* **2001**, *269*, 83−91.
(28) Voityuk, A. A.; Michel-Beyerle, M. E.; Rosch, N. *Chem. Phys. Lett.* **1997**, *272*, 162−167.
(29) Kummer, A. D.; Wiehler, J.; Rehaber, H.; Kompa, C.; Steipe, B.; Michel-Beyerle, M. E. *J. Phys. Chem B* **2000**, *104*, 4791−4798.
(30) Heikal, A. A.; Hess, S. T.; Webb, W. W. *Chem. Phys.* **2001**, *274*, 37−56.
(31) Griesbeck, O.; Baird, G. S.; Campbell, R. E.; Zacharias, D. A.; Tsien, R. Y. 2001 *J. Biol. Chem.* **276**, 29188−29194.